Journal of the Korean Society for Nondestructive Testing
Vol. 30, No. 6 (2010. 12)

Evaluation of Elastic Properties of Anisotropic Cylindrical Tubes Using an Ultrasonic Resonance Scattering Spectroscopy

Jin-Yeon Kim*† and Zheng Li**

Abstract An ultrasonic resonance scattering spectroscopy technique is developed and applied for reconstructing elastic constants of a transversely isotropic cylindrical component. Immersion ultrasonic measurements are performed on tube samples made from a boron/aluminum composite material to obtain resonance frequencies and dispersion curves of different guided wave modes propagating in the tube. Theoretical analysis on the acoustic resonance scattering from a transversely isotropic cylindrical tube is also performed, from which complete backscattering and resonance scattering spectra and theoretical dispersion curves are calculated. A sensitive change of the dispersion curves to the elastic properties of the composite tube is observed for both normal and oblique incidences; this is exploited for a systematic evaluation of damage and elastic constants of the composite tube samples. The elastic constants of two boron/aluminum composite tube samples manufactured under different conditions are reconstructed through an optimization procedure in which the residual between the experimental and theoretical phase velocities (dispersion curves) is minimized.

Keywords: Ultrasonic Spectroscopy, Elastic Constants Reconstruction, Composite Materials, Resonance Acoustic Scattering, Inverse Problem

1. Introduction

Cylindrical rods and tubes made from unidirectional fiber-reinforced composite materials are often used as an important structural component that carries a high axial load while performing their own functionalities. Efforts made in recent years have successfully led to the development of various processes to fabricate composite structures in a desired, arbitrarily-curved shape. The temperature profiles and critical pressures in the fabrication processes are the primary parameters that influence significantly the quality of composite products (Mileiko and Khvostunkov, 1995). Therefore, these parameters need to be optimized to achieve a desired product quality in terms of the fiber/matrix interface properties and the amount of inherent damage. For example, when such parameters are chosen appropriately, fiber breakage that occurs during the consolidation process is uniformly distributed, thus resulting in a minimum local damage concentration (Mileiko and Khvostunkov, 1995). The performance of such a composite fabrication process may be evaluated from the quality and properties of composite products from the process and the ultrasonic nondestructive evaluation (NDE) methods can be used for this purpose.

When the immersion ultrasonic technique is employed, the associated acoustic scattering problem needs to be analyzed for a quantitative evaluation. The acoustic scattering by an elastic cylindrical shell or tube has been a topic of

Received: October 28, 2010. Revised: December 7, 2010. Accepted: December 10, 2010. *Woodruff School of Mechanical Engineering, Georgia Institute of Technology, Atlanta, Georgia 30332, USA, **Department of Mechanics and Aerospace Engineering, Peking University, Beijing 100871, China, †Corresponding Author: jykim@gatech.edu

significant attention in many areas including underwater acoustics and NDE. Most of the previous investigations are concerned with scattering of acoustic waves by isotropic cylinders and shells. However, many engineering components are either anisotropically reinforced or can possess a certain degree of anisotropy originated from the manufacturing process. Examples include axially fiber-reinforced composite cylindrical shells and solid elastic rods that are manufactured from an extrusion process. These are the examples of cylindrical components that have the transverse isotropy. Honarvar and Sinclair (1996; 1998) studied the scattering of obliquely incident acoustic waves by a transversely isotropic solid cylinder, and examined the effect of changes in elastic constants on the resonance frequencies of the cylinder in order to characterize material properties. Niklasson and Datta (1998) analyzed the scattering of elastic waves by a transversely isotropic cylindrical inclusion in an elastic solid with another transverse isotropy. Experimental techniques for measuring acoustic resonance of immersed cylindrical objects have been well established (Ripoche et al., 1985; De Billy, 1986; Li and Ueda, 1989).

In this paper, an ultrasonic resonance scattering spectroscopy technique is developed to characterize the elastic properties of an anisotropic cylindrical component. An analysis of the associated acoustic scattering problem is conducted. Ultrasonic measurements are also performed for boron/aluminum composite tube samples manufactured under two slightly different fabrication conditions. The dispersion curves for elastic waves in the tube are obtained from the theoretical and experimental resonance frequencies in resonance backscattering spectra. The objective of the present research is to develop an experimental procedure for the reconstruction of the elastic constants from the theoretical and experimental dispersion curves. The present technique may serve as a useful tool to examine the effects of fabrication conditions on the elastic properties of the composite products.

2. Ultrasonic Experiment

Cylindrical tube samples made from a boron/aluminum unidirectional fiber-reinforced composite are used in the experiment. The tubes are fabricated such that the fiber direction of the boron/aluminum composite coincides with the cylindrical axis of the tube; samples are thus transversely isotropic with respect to the cylindrical axis. Two samples with a nominal fiber volume fraction of 20% are prepared in the process similar to the hot isostatic pressing of plasma sprayed blanks (Mileiko and Khvostunkov, 1995) under different fabrication conditions to investigate the effects of these conditions on the anisotropic elastic properties of output composite tubes. The diameter of boron fibers is about 76 μm. The outer radius of the composite tubes is 1.41 cm, the thickness 0.20 cm, and the length about 20 cm. Sample surfaces are lightly polished to remove any roughness produced during the manufacturing process.

An experimental setup for the bistatic measurement (in the pitch-catch mode) of normal and oblique scattering signals is shown in Fig. 1. The composite tube sample is immersed in a water tank and insonified with a broadband focus ultrasonic transducer (T in Fig. 1). The scattering signals are captured with a broadband ultrasonic (unfocused) transducer (R1 or R2 in Fig. 1). Both the transmitter and receiver have a center frequency 1 MHz and a frequency band 0.4-1.7 MHz. The diameter of the transducers is 38.0 mm. The angle of oblique incidence is 9°; this angle is determined such that both quasi-Lamb and quasi-SH guided waves are efficiently and simultaneously excited. As shown in Fig. 1, the resonance scattering signals are measured using the transducer R2 which is placed about 3 cm away from the point of insonification (Ripoche et al., 1985), while backscattering (specular reflection) signals are measured using

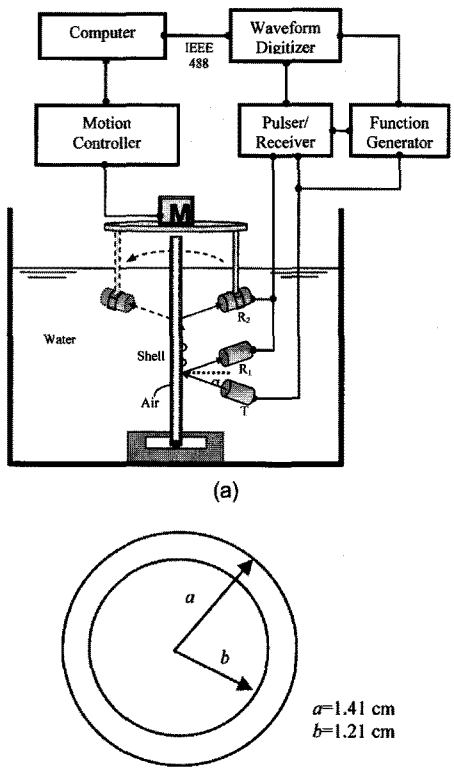

Fig. 1 Experimental setup for measuring amplitudes and directivities scattering signals at angle of α in the bistatic mode (a) and sample geometry (b)

the transducer R1. The short pulse technique (De Billy, 1986) is employed to obtain broadband backscattering and resonance scattering spectra. Then, the scattering amplitudes at different rotation angles are measured using a motor driven control system that allows for a precise rotational positioning of the receiving transducers around the tube sample. The order (n) of each resonance mode shown in the resonance spectra is determined from the number of petals within 180° in the amplitude response to tone-burst excitation (Ripoche et al., 1985). Duration of the tone-burst signals was 120 μsec.

To compensate the frequency response of both the transmitting and receiving transducers, the procedure of Li and Ueda (1989) is used. Backscattering spectra of a steel wire with

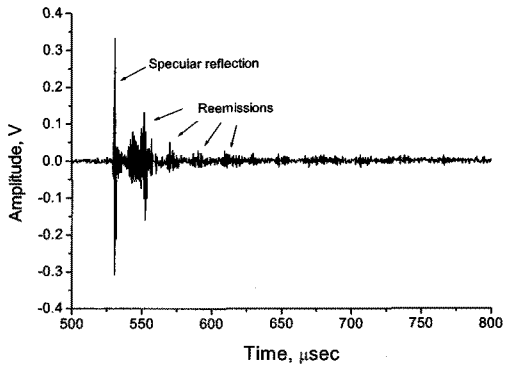

Fig. 2 Typical time domain backscattering signal from the composite tube (incident angle=9°)

0.2 mm diameter are measured using the same transducer pairs for both the normal and oblique (9°) incidences. Then, the reference spectra for the normal and oblique incidences are calculated by dividing the measured spectra with theoretical ones. Every measured spectrum is corrected by its corresponding reference spectrum. Fig. 2 illustrates a time domain backscattering signal from the boron/aluminum tube. The specular reflection and subsequent reemission signals from numerous helically-propagating elastic waves are observed as indicated by arrows in Fig. 2.

3. Theory

3.1 Scattering Analysis

Consider a transversely isotropic cylindrical tube with its axis of rotational symmetry coincident with the z-axis in the cylindrical coordinate system. The constitutive relation for such a material can be written as

$$\begin{Bmatrix} \sigma_{rr} \\ \sigma_{\theta\theta} \\ \sigma_{zz} \\ \sigma_{rz} \\ \sigma_{\theta z} \\ \sigma_{r\theta} \end{Bmatrix} = \begin{bmatrix} C_{11} & C_{12} & C_{13} & 0 & 0 & 0 \\ C_{12} & C_{11} & C_{13} & 0 & 0 & 0 \\ C_{13} & C_{13} & C_{33} & 0 & 0 & 0 \\ 0 & 0 & 0 & C_{44} & 0 & 0 \\ 0 & 0 & 0 & 0 & C_{44} & 0 \\ 0 & 0 & 0 & 0 & 0 & \dfrac{(C_{11}-C_{12})}{2} \end{bmatrix} \begin{Bmatrix} \varepsilon_{rr} \\ \varepsilon_{\theta\theta} \\ \varepsilon_{zz} \\ \gamma_{rz} \\ \gamma_{\theta z} \\ \gamma_{r\theta} \end{Bmatrix} \quad (1)$$

where σ_{ij} ($i,j=r,\theta,z$) is the stress tensor and ε_{ii} and γ_{ij} are the normal and engineering shear

components of the strain tensor; C_{ij} denotes the elastic constants in the contracted notation; five of them are independent as in eqn. (1). The cylindrical tube with density ρ and outer and inner radii a and b is immersed in a fluid of bulk modulus λ_f and density ρ_f, and the tube contains another fluid (air) of bulk modulus λ_a and density ρ_a.

A plane time-harmonic acoustic wave incident on the cylindrical tube at an oblique angle α (Fig. 1) is expressed as

$$p_i = P_o \sum_{n=0}^{\infty} \varepsilon_n i^n J_n(k_r r)\cos(n\theta)\exp(ik_z z) \quad (2)$$

where $k_r = k_f \cos\alpha$, $k_z = k_f \sin\alpha$, $\varepsilon_n = 1$ for $n = 0$ and $\varepsilon_n = 2$ for $n > 0$; $k_f (= \omega/c_f)$ is the wavenumber associated with the sound speed c_f $(= \sqrt{\lambda_f/\rho_f})$ of the surrounding fluid and $J_n(x)$ is the first kind Bessel function of order n. The time dependence $\exp(-i\omega t)$ is omitted for brevity of expression. The scattered acoustic waves that satisfy the radiation condition can be written as

$$p_s = P_o \sum_{n=0}^{\infty} \varepsilon_n i^n A_n H_n^{(1)}(k_r r)\cos(n\theta)\exp(ik_z z) \quad (3)$$

where A_n is the scattering coefficient to be determined from boundary conditions and $H_n^{(1)}(x)$ is the first kind Hankel function of order n. The acoustic field in the fluid inside the tube is

$$p_c = P_o \sum_{n=0}^{\infty} \varepsilon_n i^n K_n J_n(k_r' r)\cos(n\theta)\exp(ik_z' z) \quad (4)$$

where $k_r' = k_a \cos\alpha'$, $k_z' = k_a \sin\alpha'$, $k_a (= \omega/c_a)$ is the wavenumber associated with the sound speed $c_a (= \sqrt{\lambda_a/\rho_a})$ of the fluid and K_n is an unknown coefficient. The refraction angle α' is determined from the generalized Snell's law such that $k_z = k_z'$, and therefore,

$$\alpha' = \sin^{-1}\left(c_a/c_f \sin\alpha\right) \quad (5)$$

Likewise, the z-component wavenumbers of all associated elastic waves in the tube should be identical to that of the incident wave (k_z) again according to the generalized Snell's law.

Using the propagation constants and the formal solutions presented in Appendix, the potentials for elastic waves in the tube are represented

$$\Phi = \sum_{n=0}^{\infty} [B_n J_n(\kappa_1 r) + C_n Y_n(\kappa_1 r) + D_n J_n(\kappa_2 r) + E_n Y_n(\kappa_2 r)]\cos n\theta \exp(ik_z z) \quad (6)$$

$$\Psi = \sum_{n=0}^{\infty} [s_1 B_n J_n(\kappa_1 r) + s_1 C_n Y_n(\kappa_1 r) + s_2 D_n J_n(\kappa_2 r) + s_2 E_n Y_n(\kappa_2 r)]\cos n\theta \exp(ik_z z) \quad (7)$$

$$\Pi = \sum_{n=1}^{\infty} [F_n J_n(\kappa_3 r) + G_n Y_n(\kappa_3 r)]\sin n\theta \exp(ik_z z) \quad (8)$$

where B_n, C_n, D_n, E_n, F_n, and G_n are unknown coefficients to be determined from boundary conditions. Note that the second kind Bessel function ($Y_n(x)$) is introduced to describe the elastic wave motion in the tube thickness. The quasi-P (longitudinal) (Φ) and quasi-SV (vertically polarized shear) (Ψ) waves are coupled with each other but they are uncoupled with the quasi-SH (horizontally polarized shear) (Π) wave. The quasi-P and –SV waves forms guided waves analogous to the Lamb waves in a flat elastic plate (Gaunaurd and Werby, 1990) while the quasi-SH waves are analogous to the SH waves.

The boundary conditions on the outer tube surface $(r = a)$ are the continuity of normal displacement and normal stress, and zero shear stresses:

$$u_r\big|_{r=a} = \frac{1}{\rho_f \omega^2} \frac{\partial (p_i + p_s)}{\partial r}\bigg|_{r=a} \quad (9)$$

$$\sigma_{rr}\big|_{r=a} = -(p_i + p_s)\big|_{r=a} \quad (10)$$

$$\sigma_{\theta r}\big|_{r=a} = \sigma_{zr}\big|_{r=a} = 0 \quad (11)$$

for $0 \le \theta \le 2\pi$. Those on the inner tube surface $(r = b)$ are

$$u_r\big|_{r=b} = \frac{1}{\rho_a \omega^2} \frac{\partial p_c}{\partial r}\bigg|_{r=b} \tag{12}$$

$$\sigma_{rr}\big|_{r=b} = -p_c\big|_{r=b} \tag{13}$$

$$\sigma_{\theta r}\big|_{r=b} = \sigma_{zr}\big|_{r=b} = 0 \tag{14}$$

for $0 \le \theta \le 2\pi$. Substituting displacement and stress fields obtained from eqns. (1)-(4), eqns. (6)-(8) and the equations of motion for the exterior and interior fluids and the tube into the boundary conditions eqns. (9)-(14) yields a system of linear equations with unknown coefficients $\{A_n, B_n, C_n, D_n, E_n, F_n, G_n, K_n\}$.

The far-field scattering field can be written (Gaunaurd and Werby, 1990):

$$p_s \approx P_0 e^{i(k_f r - k_z z)} \sqrt{\frac{2}{i\pi k_f r}} \sum_{n=0}^{\infty} \varepsilon_n A_n \cos n\theta = P_0 e^{i(k_f r - k_z z)} \sqrt{\frac{a}{2r}} f_\infty(\theta) \tag{15}$$

The scattering form function $f_\infty(\theta)$ in eqn. (15) contains all the information on the acoustic properties of the scattering object. In particular, the backward and forward scattering form functions $f_\infty(\pi)$ and $f_\infty(0)$ are used in the target characterizations since none of the normal modes vanishes due to their angle dependence ($\cos n\theta$). The scattering form function is the sum of modal scattering form functions, that is,

$$f_\infty(\theta) = \sum_{n=0}^{\infty} f_n(\theta) \tag{16}$$

where

$$f_n(\theta) = \frac{2}{\sqrt{\pi k_r a}} \varepsilon_n A_n \cos(n\theta) \tag{17}$$

3.2 Reconstruction of Dispersion Curves

A direct evaluation of the dispersion characteristics of leaky elastic guided waves propagating in the circumferential direction in a fluid-loaded tube is very difficult due to the highly transcendental nature of the characteristic equations. However, the dispersion curves can be reconstructed from the resonance frequencies of the tube appearing in the backscattering signal (or in the modal backscattering form functions). To extract resonance frequencies from the modal scattering form functions, nonresonant contributions (the background), have to be known. The nonresonant contributions can be, in general, approximated with a relevant impenetrable scatterer, e.g., hard and soft scatterers for thick and very thin shells. Several models have been proposed especially for the shells that are neither thick nor thin and thus those fundamental backgrounds are not applicable (Choi et al., 1997; Yoo et al., 1998; Gaunaurd and Werby, 1990; Werby and Gaunaurd, 1986; Gaunaurd, 1992; Veksler, 1992). Recently exact backgrounds of cylindrical and spherical shells have been obtained based on the use of an absorbing scatterer (Choi et al., 1997; Yoo et al., 1998). On the other hand, it should be noted that, commonly in these different models, the background of a scatterer is independent of its elastic property of the object but depends only on the loading effects of the surrounding fluid. It can be shown that the background coefficient for the transversely isotropic tube is identical to that for an isotropic tube with the same density and thickness (Yoo et al., 1998):

$$A_n^{(b)} = \frac{F_n^{(L)}(0) J_n(k_r a) - (k_r a) J_n'(k_r a)}{(k_r a) H_n'(k_r a) - F_n^{(L)}(0) H_n(k_r a)} \tag{18}$$

where $F_n^{(L)}(0)$ denotes the zero frequency limit of modal accelerance of the equivalent liquid shell and its expression is given in (Yoo et al., 1998). The resonance form function for the n-th order normal mode is

$$f_n^{(r)}(\theta) = \frac{2\varepsilon_n}{\sqrt{\pi k_r a}} \left| (A_n - A_n^{(b)}) \cos(n\theta) \right| \tag{19}$$

Using this, resonances of elastic waves appearing in the modal backscattering form functions can be isolated and characterized. Once the resonance frequency in the n-th order partial scattering form function (in terms of $(k_r a)_n$) is obtained, the phase velocity of the wave mode that produces the resonance can be calculated by

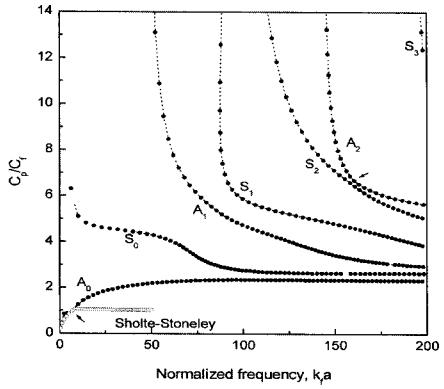

Fig. 3 Dispersion curves for propagating waves excited by normally incident acoustic wave

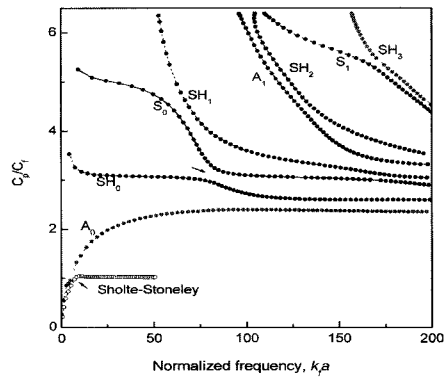

Fig. 4 Dispersion curves for propagating waves excited by normally incident acoustic wave

Table 1 Elastic constants (GPa) and density (kg/m^3) of materials

Material	C_{11}	C_{12}	C_{13}	C_{33}	C_{44}	Density
Boron/aluminum composite (theoretical)	142.1	71.1	66.4	219.4	37.1	2738
Material	λ					Density
Water	2.16					1000
Air	0.00013					1.2

the following formula for a given incident angle (α):

$$c_p = c_f / \sqrt{[n/(k_r a)_n]^2 + \sin^2 \alpha} \qquad (20)$$

4. Results and Discussion

Numerical calculations have been performed to characterize dispersive characteristics of the elastic waves in the boron/aluminum cylindrical tube and to identify the resonance modes in the experimental results. The nominal elastic properties of the composite tube and those of the water and the air used in the calculation are presented in Table 1. The higher order Bessel functions (up to n=125) are calculated using the commercial software Mathematica®.

The dispersion curves of resonant wave modes for the normal incidence ($\alpha = 0^\circ$) are shown in Fig. 3. The modes of wave propagation shown as trajectories of the resonance frequencies are marked. The fluid-borne Sholte-Stoneley and quasi-Lamb wave modes are observed. Note that all these guided waves propagate only in the circumferential direction. Due to the curvature of the tube, the phase velocity of the S_0 mode in the low frequency limit does not remain finite.

The dispersion curves for 9° incidence are shown in Fig. 4. The behavior of the Sholte-Stoneley wave mode remains the same as in the normal incidence case due to its fluid-borne nature. The guided waves excited by the obliquely (9°) incident acoustic wave propagate along helical paths in the cylindrical tube. The additional quasi-SH wave modes (Maze et al., 1985; Conoir et al., 1993) (marked SH_n) are also observed. The SH wave modes can be useful to measure elastic properties and/or material damage in the axial direction. The shift of dispersion curves due to the oblique excitation is noted. The repulsion of dispersion curves of the Sholte-Stoneley and A_0 modes in the low frequency region is observed (marked with arrows) (Überall, et al., 1994): the dispersion curves for a fluid-loaded elastic object do not cross. The repulsions between the Lamb and SH waves as well as between different

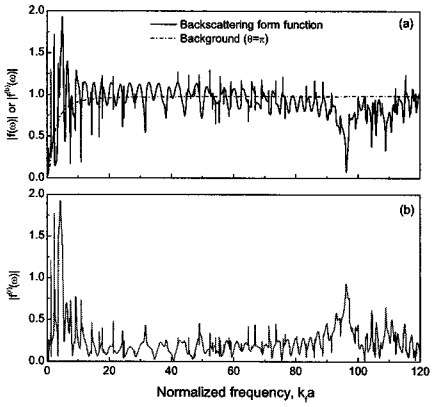

Fig. 5 (a) Backscattering, background and (b) Complete resonance form functions for oblique (9°) incidence

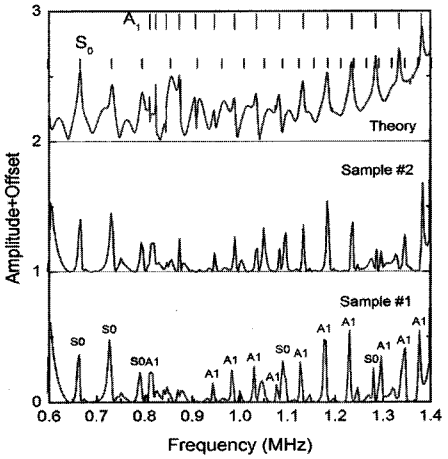

Fig. 6 Comparison of resonance spectra from theory with those from experiments for different samples (scattering for normal incidence)

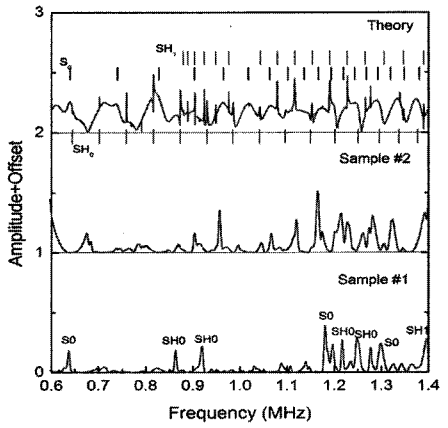

Fig. 7 Comparison of resonance spectra from theory with those from experiments for different samples (scattering for incident angle 9°)

Lamb waves are also seen in Figs. 3 and 4.

In Fig. 5, the theoretical backscattering and resonance form functions for 9° incidence are shown. Note that the theoretical curves are calculated using the material properties shown in Table 1. Referring to the dispersion curves in Fig. 4, the number of partial waves required to calculate the these spectra is $N > k_f a$. Strong resonances of the A_0 Lamb wave are seen in the low frequencies. The complete resonance form function is obtained by subtracting the background from the backscattering form function as shown in Fig. 5(b).

The calculated resonance spectra are compared with experimental ones for the two samples in Figs. 6 and 7. Some resonances frequencies of quasi-SH and Lamb waves are indicated. It is known that elastic properties of a composite tube are significantly influenced by the fabrication conditions. In general, the backscattering spectra from the theory and experiment are in good agreement. The Sholte-Stoneley wave resonances are not clearly seen in the experimental resonance spectra because of their high radiation damping in fluid. The downward shifts of resonance frequencies are noted in these figures. It is not easy to track the exact correspondence between theoretical and experimental resonance frequencies in these spectra. Nevertheless, once the order n of each resonance mode is identified from the rotational measurements, the phase velocity (and the propagation mode) of the associated elastic wave can be determined using eqn. (20).

In Figs. 8 and 9, the resonance frequencies identified from the tone-burst experiments are compared with those from the numerical calculations. Shifts of the resonance frequencies are clearly seen in these figures. Figure 8 shows that resonance frequencies for sample #2 shift

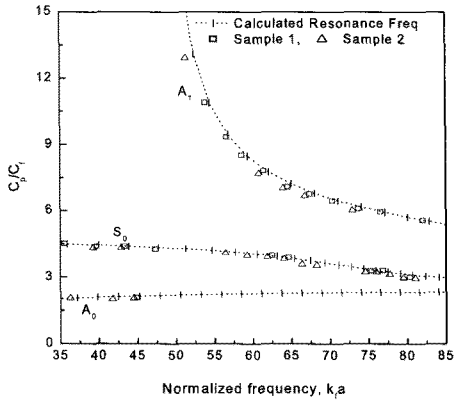

Fig. 8 Comparison of resonance frequencies of samples (for normal incidence) from experiments and calculation

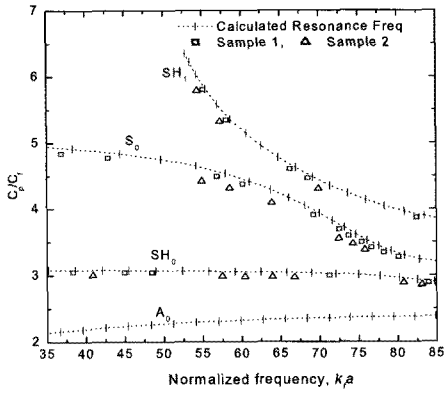

Fig. 9 Comparison of resonance frequencies of samples (for oblique incidence) from experiments and calculation

Table 2 Reconstructed elastic constants (GPa) of the two composite tube samples

Material	C_{11}	C_{12}	C_{13}	C_{33}	C_{44}
Sample #1	128.8±3.0	64.7±1.9	60.1±0.8	209.7±7.4	33.7±0.9
Sample #2	132.0±2.1	64.5±2.2	60.3±1.8	211.8±6.8	35.4±2.2

less than those for sample #1. Assuming that the manufacturing damage reduces the stiffness and the resonance frequencies of the tube, it can be said that the sample #2 is less damaged than the other in the basal plane. Also, in Fig. 9 for the oblique incidence, it is observed that sample #2 exhibits a less downward shift of the resonance frequencies than the sample #1. Since elastic constants are related directly to resonance frequencies, they can be reconstructed from resonance frequencies (Honarvar and Sinclair, 1996; 1998). A reconstruction method has been developed that uses the dispersion curves of multiple wave modes obtained from the ultrasonic measurements as shown in Figs. 8 and 9. The inversion of the elastic constants is performed by solving a multi-variate optimization problem in which the sum of square errors between experimental and theoretical dispersion curves is minimized (Kim and Rokhlin, 2009):

$$\underset{C_{ij}}{\text{Min}} \sum_{n} \left(c_p^{Exp}(n) - c_p^{Theory}(C_{ij}, n) \right)^2 \qquad (21)$$

The reconstruction is based on the guided wave dispersion curves measured from the experiment and predicted by the theoretical model. The experimentally determined guided wave velocities for different modes are used in the reconstruction procedure. The optimization algorithm updates the five elastics until the error function in eqn. (21) is minimized. The simultaneous use of dispersion curves obtained from normal and oblique scattering measurements offers a systematic method for assessing the damage (or elastic constants) both in the lateral and axial directions. The selection of modes is important in that the excited modes should be measurable in the frequency range and they should be sensitive to the particular damage or elastic constants of interest. In Table 2, the reconstructed elastic constants of the two samples (an average from three measurements) together with maximum error ranges are shown.

5. Summary

An ultrasonic resonance scattering spectroscopy technique is developed and applied for quantitative evaluation of elastic constants of a transversely isotropic cylindrical component. Immersion ultrasonic measurements are performed on tube samples made from boron/aluminum composite material to obtain resonance frequencies and dispersion curves of different elastic guided wave modes propagating in the tube. The theoretical analysis is performed on the acoustic resonance scattering from a transversely isotropic cylindrical tube. For two composite tube samples fabricated under different conditions, elastic constants are reconstructed using the experimental and theoretical dispersion curves through an optimization procedure in which the residual between experimental and theoretical phase velocities of different guided wave modes is minimized. A sensitive change of the dispersion curves to the elastic properties of the tube is observed for both normal and oblique incidences and therefore the developed method can be used for evaluating damage or elastic constants of the composite tube and shell samples.

References

Auld, B. A. (1973) *Acoustic Fields and Waves in Solids*, John Wiley & Sons, New York

Choi, M. S., Joo, Y.-S. and Lee, J.-P. (1997) Inherent Background Coefficients for Submerged Cylindrical Shells, *J. Acoust. Soc. Am.* 101, pp. 1743-1745

Conoir, J. M., Rambert, P., Lenoir, O. and Izbicki, J. L. (1993) Relation between Surface Helical Waves and Elastic Cylinder, *J. Acoust. Soc. Am.* 93, pp. 1300-1307

De Billy, M. (1986) Determination of the Resonance Spectrum of Elastic Bodies via the Use of Short Pulses and Fourier Transform Theory, *J. Acoust. Soc. Am.* 79, pp. 219-221

Gaunaurd, G. C. and Werby, M. F. (1990) Acoustic Resonance Scattering by Submerged Elastic Shell, *Appl. Mech. Rev.* 43, pp. 171-208

Gaunaurd, G. C. (1992) Hybrid Background Coefficients to Isolate the Resonance Spectrum of Submerged Shells, *J. Acoust. Soc. Am.* 92, pp. 1981-1984

Honarvar, F. and Sinclair, A. N. (1996) Acoustic Wave Scattering from Transversely Isotropic Cylinders, *J. Acoust. Soc. Am.* 100, pp. 57-63

Honarvar, F. and Sinclair, A. N. (1998) Nondestructive Evaluation of Cylindrical Components by Resonance Acoustic Spectroscopy, *Ultrasonics 36*, pp. 845-854

Joo, Y.-S., Ih, J.-G. and Choi, M.-S. (1998) Inherent Background Coefficients for Acoustic Resonance Scattering from Submerged, Multilayered, Cylindrical Structures, *J. Acoust. Soc. Am.* 103, pp. 900-910

Kim, J.-Y. and Rokhlin, S.I. (2009) Determination of Elastic Constants of Generally Anisotropic Inclined Lamellar Structure Using Line-Focus Acoustic Microscopy, *J. Acoust. Soc. Am.* 126, pp. 2998-3007

Li, T.-B. and Ueda, M. (1989) Sound Scattering of a Plane Wave Obliquely Incident on a Cylinder, *J. Acoust. Soc. Am.* 86, pp. 2363-2368

Maze, G., Izbicki, J. L. and Ripoche, J. (1985) Resonances of Plates and Cylinders: Guided waves, *J. Acoust. Soc. Am.* 77, pp. 1352-1357

Mileiko, S. T. and Khvostunkov, A. A. (1995) Boron/Aluminium Shells Under Hydrostatic Pressure, *Composites Science and Technology*, 55, pp. 25-32

Morse, P. M. and Feshbach, H. (1953) *Methods of Theoretical Physics*, McGraw-Hill, New York

Niklasson, A. J. and Datta, S. K. (1998) Scattering by an Infinite Transversely Isotropic Cylinder in a Transversely Isotropic Medium, *Wave Motion* 27, pp. 169-185

Ripoche, J., Maze, G. and Izbicki, J.-L. (1985) A New Acoustic Spectroscopy: Resonance Spectroscopy by the MIIR, *J. of Nondestruct. Eval.* 2, pp. 69-79

Überall, H., Hosten, B., Deschamps, M. and Gerard, A. (1994) Repulsion of Phase-Velocity Dispersion Curves and the Nature of Plate Vibrations, *J. Acoust. Soc. Am.* 94, pp. 908-917

Veksler, D. N. (1992) Intermediate Background in Problems of Sound Waves Scattering by Elastic Shells, Acustica 76, pp. 1-9

Werby, M. F. and Gaunaurd, G. C. (1986) Transition from Soft to Rigid Behavior in Scattering from Submerged Thin Elastic Shells, *Acoust. Lett.* 9, pp. 89-93

Appendix

The elastic displacement vector in the cylindrical coordinate system can be represented by three scalar potentials, Φ, Ψ, and Π that satisfy scalar wave equation (Morse and Feshbach, 1953),

$$\mathrm{u} = \nabla\Phi + l\nabla\times\nabla\times(\Psi\hat{\mathrm{z}}) + \nabla\times(\Pi\hat{\mathrm{z}}) \qquad \text{(A1)}$$

where $\hat{\mathrm{z}}$ is the unit vector in z-direction. The constant l has the dimension of length and is introduced for equidimensionality, and is set to be $l = k_z^{-1}$.

In order to obtain propagation constants (wavenumbers) in r-direction for propagating wave modes, the potentials are assumed in the following forms,

$$\Phi = B_n X_n(\kappa r)\cos n\theta \exp[\,i(k_z z - \omega t)] \qquad \text{(A2)}$$

$$\Psi = C_n X_n(\kappa r)\cos n\theta \exp[\,i(k_z z - \omega t)] \qquad \text{(A3)}$$

$$\Pi = D_n X_n(\kappa r)\sin n\theta \exp[\,i(k_z z - \omega t)] \qquad \text{(A4)}$$

where X_n denotes the relevant kind of Bessel functions of order n. Substituting eqns. (A2)-(A4) into the equations of motion for transversely isotropic solid yields the Chrstoffel matrix (Auld, 1973) for the quasi-P and -SV waves:

$$\begin{vmatrix} \rho\omega^2 - C_{11}\kappa^2 - (C_{13}+2C_{44})k_z^2 & i\{\rho\omega^2 - C_{44}k_z^2 - (C_{33}-C_{13}-C_{44})\kappa^2\} \\ ik^2\{\rho\omega^2 - C_{33}k_z^2 - (C_{13}+2C_{44})\kappa^2\} & \kappa^2\{\rho\omega^2 - C_{44}\kappa^2 - (C_{33}-C_{13}-C_{44})k_z^2\} \end{vmatrix} = 0 \qquad \text{(A5)}$$

Two roots κ_1 and κ_2 (so to say $\kappa_2 > \kappa_1$) of eqn. (A5) correspond to the wavenumbers of the quasi-P and quasi-SV waves, respectively. Then, the coupling coefficient is

$$s_{1,2} = \frac{i\left[\rho\omega^2 - C_{11}\kappa_{1,2}^2 - (C_{13}+2C_{44})k_z^2\right]}{\left[\rho\omega^2 - C_{44}k_z^2 - (C_{11}-C_{13}-2C_{44})\kappa_{1,2}^2\right]} \qquad \text{(A6)}$$

Therefore, the potentials have the following forms

$$\Phi = \sum_{n=0}^{\infty}\left[B_n X_n(\kappa_1 r) + C_n X_n(\kappa_2 r)\right]\cos n\theta \exp[i(k_z z - \omega t)] \qquad \text{(A7)}$$

$$\Psi = \sum_{n=0}^{\infty}\left[s_1 B_n X_n(\kappa_1 r) + s_2 C_n X_n(\kappa_2 r)\right]\cos n\theta \exp[i(k_z z - \omega t)] \qquad \text{(A8)}$$

The characteristic equation for the quasi-SH wave is

$$\frac{C_{11} - C_{12}}{2}\kappa^2 + C_{44}k_z^2 - \rho\omega^2 = 0 \qquad \text{(A9)}$$

which gives wavenumber κ_3 and the potential in the following form

$$\Pi = \sum_{n=0}^{\infty} D_n X_n(\kappa_3 r)\sin n\theta \exp[i(k_z z - \omega t)] \qquad \text{(A10)}$$